



TÉCNICA FOTOTÉRMICA PARA A MEDIÇÃO DA CONDUTIVIDADE TÉRMICA E A DIFUSÃO DE NANOFLUIDOS: UMA NOVA ABORDAGEM



PHOTOTHERMAL TECHNIQUE FOR MEASURING THERMAL CONDUCTIVITY AND DIFFUSIVITY OF NANOFLUIDS: A NEW APPROACH

HECHAVARRÍA, Rodney^{1*}; DELGADO, Osvaldo²; HIDALGO, Andrés³; ESPÍN, Segundo⁴;
GUAMANQUISPE, Jorge⁵

^{1,3,4,5} Technical University of Ambato, Campus Huachi, Los Chasquis and Río Payamino, Ambato, Ecuador
(phone: +593 3 2841144)

² Metropolitan Polytechnic University of Hidalgo, Boulevard Acceso a Tolcayuca # 1009 Ex Hacienda de San
Javier, Tolcayuca, México
(phone: + 743 7411015)

* *Autor correspondente*
e-mail: ro.hechavarría@uta.edu.ec

Received 08 December 2017; accepted 09 December 2017

RESUMO

Os nanofluidos tornaram-se hoje em dia de especial importância por causa de seus diferentes usos na indústria, portanto, propor métodos para calcular suas propriedades térmicas seriam úteis. Neste trabalho, propõe-se uma nova variante para o cálculo da condutividade térmica e difusividade de nanofluidos; são estudadas as possibilidades e limitações desse método não estacionário, que utiliza a radiação de luz como fonte de calor. Aqui, a luz é incidente homogêneo em uma das superfícies de extremidade de um cilindro que tem uma superfície lateral isolada termicamente, ajustando a temperatura na outra extremidade para um valor constante, então a distribuição da temperatura é obtida em função da coordenada e do tempo; ajustando o modelo teórico, a equação de difusão de calor parabólico, aos dados experimentais obtidos. São analisadas as condições de validade do método para medir a difusividade térmica e a condutividade térmica dos fluidos; bem como a forma como ele poderia ser usado para verificar a validade do modelo de Hamilton e Crosser (HC) no caso dos nanofluidos. Atualmente, os nanofluidos são usados para trocar calor, pois verificaram-se que excedem o potencial dos refrigerantes convencionais; no entanto, o cálculo de propriedades térmicas ainda não oferece valores definitivos.

Palavras-chave: condutividade térmica, difusividade térmica, modelo Hamilton e Crosser, nanofluidos.

ABSTRACT

Nanofluids have become nowadays of special importance because of their different uses in industry, therefore, to propose methods to calculate their thermal properties would be useful. In this work, a new variant for the calculation of thermal conductivity and diffusivity of nanofluids is proposed; the possibilities and limitations of this non-stationary method, which uses light radiation as the heat source, are studied. Here, the light is homogeneously incident on one of the end surfaces of a cylinder that has a thermally insulated side surface, setting the temperature at the other end to a constant value, then the temperature distribution is obtained as a function of the coordinate and time; adjusting the theoretical model, parabolic heat diffusion equation, to the experimental data obtained. The conditions of validity of the method to measure thermal diffusivity and thermal conductivity of fluids are analyzed; as well as, the way in which it could be used to verify the validity of the Hamilton and Crosser (HC) model in the case of nanofluids. Currently, nanofluids are used to exchange heat, as they have been found to exceed the potential of conventional refrigerants; however, the calculation of thermal properties still does not offer definitive values.

Keywords: thermal conductivity, thermal diffusivity, Hamilton and Crosser model, nanofluids.

INTRODUCTION

At present, several methods are known to determine the thermal conductivity and diffusivity of materials (Fox and McMaster, 1975; Ficker, 1996; Hurley *et al.*, 2015; Keblinski *et al.*, 2002; Xue and Xu, 2005; Gregorová, 2014; Xuan and Li, 2000; Putnam *et al.*, 2006), (González *et al.* 2014; Warriar *et al.* 2015; Martínez *et al.* 2015; Cobirzan *et al.* 2016). Therefore, choosing the appropriate method in each particular situation is of great importance. To do this it is necessary to take into account several factors.

- 1) If high precision is not required, then very sophisticated methods are unnecessary.
- 2) Stationary methods are usually time consuming and therefore not suitable for measuring large numbers of samples.
- 3) If it is not possible to prepare specimens of defined geometry, methods using point and linear sources should be preferred.

All the methods used to measure thermal properties can be divided into two fundamental groups: I) methods that use heat sources and II) those that do not. In the latter group the temperature T of the medium is modulated by contact with an infinite heat exchanger, while in the first the heat source acts on the inside of the sample or on its surface.

Methods that do not use heat sources can be divided into stationary and non-stationary. For their part, methods that use heat sources are also divided into stationary and non-stationary; But in this case other classification factors become more important, namely: a) the geometry of the source (punctual, linear, superficial or volumetric), b) the temporal dependence of the power source (pulse rate or continuous) and c) the configuration of the sample being measured (eg plane-parallel, cylindrical or spherical). Since each experimental setup can employ several combinations of the three groups a) - c) there are a large number of modifications, each of which requires its particular solution $T(x, y, z, t)$ of the Heat diffusion equation (Ficker, 1996).

The present work aims to study the possibilities and limitations of a non-stationary method, which uses light radiation as a source of heat. In this method, which is a new proposed variant, the light is homogeneously placed on one of the end surfaces of a cylinder, which, under vacuum, would not have convective heat transfer.

In a non-stationary state the temperature hardly varies due to radiation either; keeping the temperature constant at the other end.

There are several theoretical models such as Hamilton and Crosser (HC) that predict the behavior of the thermal conductivity of the compounds and mixtures according to the proportion of the components that form it (Maxwell, 1881). However, in spite of the fact that they have successfully withstood multiple experimental tests, in the last years a great discussion has arisen as to their validity when it comes to nanofluids (Hurley *et al.*, 2015; Keblinski *et al.*, 2002; Xue and Xu, 2005; Gregorová, 2014; Xuan and Li, 2000; Shemeena, 2012).

The controversy, as yet unresolved, about the validity of the HC model, as well as of other equivalents (Xue and Xu, 2005;), arises because the measurements of thermal conductivity that have been realized on these systems reveal values that far surpass those that predict said Models (Keblinski *et al.*, 2002; Xue and Xu, 2005; Gregorová, 2014). To date, there is an insufficient amount of experimental data and the vast majority of it has been obtained using a single method, the hot wire method (Putnam *et al.*, 2006; Eastman *et al.*, 2001; Choi *et al.*, 2001; Xie *et al.*, 2002; Klingenberg and Venerus, 2006). In turn, other measurements obtained using different methods yield conflicting results with those reported initially (Zhang *et al.*, 2006).

In conclusion, it can be inferred that either a new theory needs to be developed or the thermal conductivity values reported do not reflect reality. The latter may be due to several factors that have not been taken into account when taking and interpreting the measurements.

MATERIALS AND METHODS

The proposed experimental method consists of the following (Figure 1a and 1b): If the material to be studied is a homogeneous and transversely isotropic metallic solid, then a cylindrical rod must be prepared of it. This rod is placed inside a vacuum chamber for the purpose of preventing heat exchange, by conduction and convection, through its front and side surfaces. The back surface of the bar is fixed to the wall of the chamber so that, on that surface, the temperature remains constant. This can be achieved with a large base preferably of copper.

If the sample is a fluid, a cylindrical vessel must be prepared, at the front end of which, in direct contact with the sample, a sheet of aluminum or other solid material with good heat transfer is attached where the light strikes. The other end of said container will be attached, as in the case of solid samples, to the wall of the vacuum chamber, which in this case will have an aperture to allow the fluid to enter.

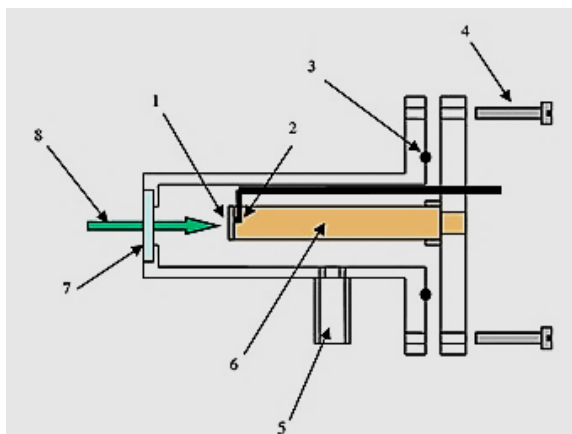


Figure 1a. The figure represents a scheme of the device that is proposed to measure the thermal conductivity and diffusivity of solids. 1. Front surface. 2. Thermocouple. 3. O-Ring. 4. Screws. 5. Vacuum inlet. 6. Sample. 7. Glass window. 8. Light (not modulated)

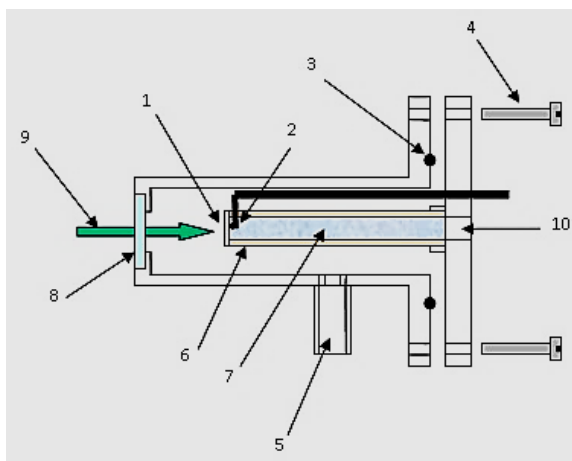


Figure 1b. The figure represents a scheme of the device that is proposed to measure thermal conductivity and diffusivity of fluids. 1. Al sheet. 2. Thermocouple. 3. O-Ring. 4. Screws. 5. Vacuum inlet. 6. Showcase. 7. Sample. 8. Glass window. 9. Light (not modulated). 10. Opening to enter the sample.

2.1. Theoretical model

2.1.1 Problem Statement

Heat always propagates from areas of greater to lower temperatures. Three forms of heat propagation are distinguished: conduction, convection and radiation.

As in the model (Figure 2), a solid homogeneous cylindrical rod with the length l , the area of its cross-section A , the lateral surfaces $x = L$ through which it is impossible to exchange heat by conduction or convection, the back surface $x = 0$ and is maintained at a constant temperature Ω_0 , which coincides with the initial temperature of the entire rod, is made. It is assumed that the power of the heat source q is distributed homogeneously on the front surface, above which the light radiation is incident, and that the heat loss by radiation is negligible. Under these conditions we can consider that we are in the presence of a one-dimensional problem and, therefore, the heat diffusion equation is in one direction.



Figure 2. Solid cylindrical bar with adiabatic lateral walls

$$\frac{\partial \Omega(x,t)}{\partial t} = a \frac{\partial^2 \Omega(x,t)}{\partial x^2} + F(x,t) \quad (\text{Eq. 1})$$

In (1) α is the thermal diffusivity, given by $a = \frac{\chi}{\rho c}$ where ρ is density, c specific heat, $F(x, t)$

t) considers the internal heat sources and is equal to $F(x,t) = \frac{Q(x,t)}{\rho c}$, where $Q(x, t)$ is the

density of internal heat sources. In this model, no internal sources of heat are contemplated, since it is generated homogeneously on the surface. Therefore, the equation (1) to be solved is reduced to:

$$\frac{\partial \Omega(x,t)}{\partial t} = a \frac{\partial^2 \Omega(x,t)}{\partial x^2} \quad (\text{Eq. 2})$$

whose initial conditions and frontiers are as follows:

$$\begin{aligned}\Omega(x, 0) &= \Omega_0 \\ \Omega(0, t) &= \Omega_0, \quad \forall 0 < x < l, t > 0 \\ \frac{\partial \Omega(l, t)}{\partial x} &= Q\end{aligned}\quad (\text{Eq. 3})$$

where: $Q = \frac{q}{\chi A}$, and q is the heat flux through the front surface of the sample, which is considered constant (q depends directly on the intensity of light coming from the source of illumination), χ is the thermal conductivity and A , the cross-sectional area of the sample. The solution of this problem is proposed as:

$$\Omega(x, t) = v(x, t) + p(x) \quad (\text{Eq. 4})$$

Substituting (4) into the equation (2) gives the following expression:

$$\frac{\partial v(x, t)}{\partial t} = \alpha \frac{\partial^2 v(x, t)}{\partial x^2} + \alpha \frac{d^2 p(x)}{dx^2} \quad (\text{Eq. 5})$$

This leads us to two new equations, the first for $p(x)$ and the second for $v(x, t)$.

$$\frac{d^2 p(x)}{dx^2} = 0 \quad (\text{Eq. 6})$$

border conditions:

$$\begin{aligned}\frac{dp}{dx}(l) &= Q \\ p(0) &= \Omega_0\end{aligned}\quad (\text{Eq. 7})$$

Equation (6) is an ordinary differential equation with constant coefficients, the solution of which can be obtained in the form:

$$p(x) = Qx + \Omega_0 \quad (\text{Eq. 8})$$

For $v(x, t)$ we have:

$$\frac{\partial v(x, t)}{\partial t} = \alpha \frac{\partial^2 v(x, t)}{\partial x^2} \quad (\text{Eq. 9})$$

border conditions:

$$\begin{aligned}v(0, t) &= 0 \\ \frac{\partial v(l, t)}{\partial x} &= 0\end{aligned}\quad (\text{Eq. 10})$$

By the method of separating variables, in partial derivatives, we look for the solution of this equation in the form:

$$v(x, t) = U(t) \cdot X(x) \neq 0 \quad (\text{Eq. 11})$$

$$\frac{dU(t)}{dt} + \alpha \lambda U(t) = 0 \quad (\text{Eq. 11.1})$$

Equation (11.1) is an ordinary differential equation and its solution is:

$$U(t) = C \cdot e^{-\lambda \cdot \alpha t} \quad (\text{Eq. 11.2})$$

where: C is an arbitrary constant. For the spatial part we obtain:

$$\frac{d^2 X}{dx^2} + \lambda X(x) = 0 \quad (\text{Eq. 11.3})$$

whose initial and boundary conditions are:

$$\begin{aligned}X(0) &= 0 \\ \frac{dX}{dx}(l) &= 0, \quad \forall 0 < x < l \\ X(x) &\neq 0\end{aligned}\quad (\text{Eq. 11.4})$$

The general solution of this problem is:

$$X(x) = D \text{sen}(\sqrt{\lambda} x) + B \text{cos}(\sqrt{\lambda} x) \quad (\text{Eq. 11.5})$$

Imposing that (11.5) satisfies (11.4), we will have:

$B = 0$ and the eigenvalues: $\lambda_n = \left[(2n+1) \frac{\pi}{2l} \right]^2$, $n = 0, 1, 2, 3 \dots$. Therefore, the solution of Equation (11.3) will be:

$$X_n(x) = D \text{sen} \left[(2n+1) \frac{\pi x}{2l} \right] \quad (\text{Eq. 11.6})$$

where: D is an arbitrary constant, hence the general solution of equation (9) without considering the initial conditions can be written as:

$$v(x, t) = \sum_{n=0}^{\infty} C_n \cdot e^{-\left[\frac{(2n+1)\pi}{2l} \right]^2 \alpha t} \text{sen} \left[\frac{(2n+1)\pi x}{2l} \right] \quad (\text{Eq. 12})$$

The constant C_n is determined by imposing on the function (12) the fulfillment of the initial condition:

$$v(x, 0) = \sum_{n=0}^{\infty} C_n \text{sen} \left[(2n+1) \frac{\pi x}{2l} \right] = \Omega_0 - p(x) = \varphi(x)$$

(Eq. 13)

wherein:

$$C_n \equiv \varphi_n = \frac{2}{l} \int_0^l \varphi(\xi) \text{sen} \left[(2n+1) \frac{\pi \xi}{2l} \right] d\xi$$

(Eq. 14)

Substituting (14) into (12) we obtain:

$$v(x, t) = \sum_{n=0}^{\infty} \frac{2}{l} \int_0^l \varphi(\xi) \cdot \text{sen} \left[\frac{(2n+1)\pi \xi}{2l} \right] d\xi \cdot e^{-\left[\frac{(2n+1)\pi}{2l} \right]^2 \alpha t} \cdot \text{sen} \left[\frac{(2n+1)\pi x}{2l} \right]$$

(Eq. 15)

Introducing the notation:

$$G(x, \xi, t) = \sum_{n=0}^{\infty} \frac{2}{l} \text{sen} \left[\frac{(2n+1)\pi \xi}{2l} \right] \cdot e^{-\left[\frac{(2n+1)\pi}{2l} \right]^2 \alpha t} \cdot \text{sen} \left[\frac{(2n+1)\pi x}{2l} \right]$$

(Eq. 16)

The solution if equation (15) is:

$$v(x, t) = \int_0^l G(x, \xi, t) \cdot \varphi(\xi) d\xi \quad (\text{Eq. 17})$$

The function (16) is the Green function of the problem. If we integrate, there is:

$$v(x, t) = \frac{-8lQ}{\pi^2} \sum_{n=0}^{\infty} \frac{(-1)^n}{(2n+1)^2} \cdot e^{-\left[\frac{(2n+1)\pi}{2l} \right]^2 \alpha t} \cdot \text{sen} \left[\frac{(2n+1)\pi x}{2l} \right]$$

(Eq. 18)

Considering (4) we finally arrived at:

$$\Omega(x, t) = \Omega_0 + Qx - \frac{8lQ}{\pi^2} \sum_{n=0}^{\infty} \frac{(-1)^n}{(2n+1)^2} \cdot e^{-\left[\frac{(2n+1)\pi}{2l} \right]^2 \alpha t} \cdot \text{sen} \left[\frac{(2n+1)\pi x}{2l} \right]$$

(Eq. 19)

This expression can be written as:

$$T(x, t) = T_{es} \left\{ \frac{x}{l} - \frac{8}{\pi^2} \sum_{n=0}^{\infty} \frac{(-1)^n}{(2n+1)^2} \cdot e^{-t/\tau} \cdot \text{sen} \left[\frac{(2n+1)\pi x}{2l} \right] \right\}$$

(Eq. 20)

where:

$$T_{es} = \frac{ql}{\chi A} \quad (\text{Eq. 21})$$

is the temperature corresponding to the steady state at the position $x = 1$, while:

$$\tau = \frac{1}{\left[\frac{(2n+1)\pi}{2l} \right]^2 \alpha} \quad (\text{Eq. 22})$$

is the time during which the temperature $T(x, t)$ reaches the value:

$$T(x, t) = T_{es} \left\{ \frac{x}{l} - \frac{8}{\pi^2} \sum_{n=0}^{\infty} \frac{(-1)^n}{(2n+1)^2} \cdot e^{-t/\tau} \cdot \text{sen} \left[\frac{(2n+1)\pi x}{2l} \right] \right\} \quad (\text{Eq. 23})$$

Expression (20) represents the increase in temperature relative to the initial temperature while generating heat at the surface of the sample.

2.2. Applicability of the fluid model

Although the heat diffusion equation (1), in general, is not valid for the case of fluids, it can be applied to these when the phenomenon of convection inside them is negligible.

On the other hand, the fluids must be contained in some container, which in our case is the sample holder. This causes the thermal diffusivity and conductivity values in expression (20) and, which can be measured in the experiment, to be actually the effective values of the system composed of the sample holder plus the fluid. That is, they are magnitudes that take into account the characteristics of both of them.

Thus, for the effective thermal conductivity and diffusivity, we have the following expressions (Hamilton and Crosser, 1962):

$$\chi_{ef} = \mu \cdot \chi_f + (1 - \mu) \cdot \chi_p$$

$$\alpha_{ef} = \frac{\mu \cdot \chi_f + (1 - \mu) \cdot \chi_p}{\mu \cdot \rho c_f + (1 - \mu) \cdot \rho c_p} \quad (\text{Eq. 24})$$

where: μ is the cross-sectional area ratio, which includes the sample holder in the system, ρ is the density of each material and the subscripts f and p represent the fluid and the sample holder respectively.

2.3. Temporal variation of temperature

Figure 3 graphically shows the temperature behavior on the front surface of a liquid sample, as indicated in Figure 1b, of distilled water. In this graph we can observe that while the light falls on the sample, the temperature rises to reach a constant value. From the moment a steady state is entered, the temperature no longer increases, reaching the value given by (21); hence we see that the saturation temperature T_e depends on the power of the heat source at the surface, the length of the sample, its cross-section area and the thermal conductivity thereof.

In Figure 3 it is observed that the saturation temperature of the sample reaches a value of about 28 °C. In practice it is necessary to limit the rise in temperature since on the one hand the thermal properties of the sample would vary during the measurements, and on the other, the heat loss caused by the radiation mechanism would be important. This would imply that the real behavior of the system does not correspond to what the theoretical model predicts. For this reason, depending on the thermal conductivity values of the sample, it is necessary to choose the values of the other three quantities involved in the expression adequately (21). This choice must be made considering that the time during which it is measured should be enough to obtain a number of experimental points which would allow the subsequent determination of the magnitudes sought.

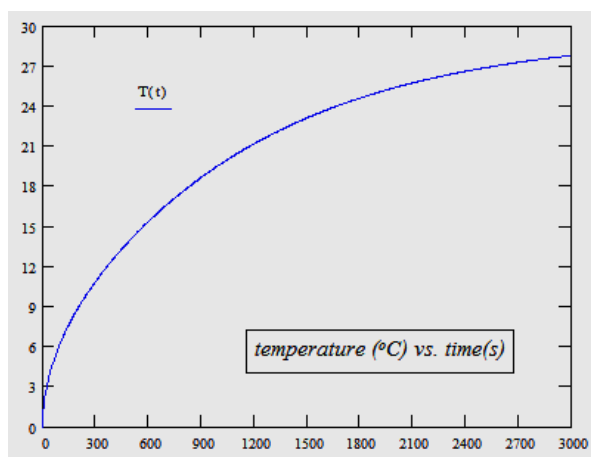


Figure 3. Temporal dependence of temperature on the frontal surface ($x = l$), for values of, $q = 0.1$ W, $l = 0.02$ m, $A = 1,131 \times 10^{-4}$ m², $\chi = 0.599$ W/m °C, $\alpha = 1.430 \times 10^{-7}$ m²/s, corresponding to a liquid sample of distilled water.

RESULTS AND DISCUSSION

3.1. Resolution of the method

Figure 4 shows, graphically, the temperature difference as a function of time $\Delta T(t)$ when the thermal conductivity value varies by 5%. While in figure 5, it is shown how the temperature $T(t)$ varies as a function of time for two samples whose thermal conductivities differ from each other by 5%.

For a given variation of the thermal conductivity, more time and greater temperature differences are needed. That is, as the resolution of the method increases, it will be possible to detect smaller differences in thermal conductivity using the same temperature sensor.

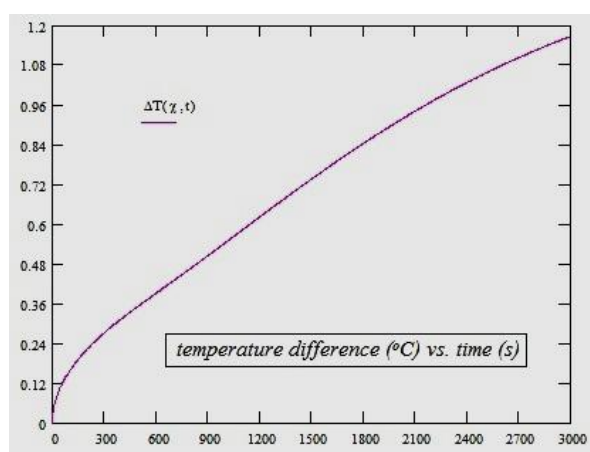


Figure 4. Temperature difference as a function of time for values of, $q = 0.1$ W, $l = 0.02$ m, $A = 1,131 \times 10^{-4}$ m², $\chi = 0.599$ W/m °C, $\alpha = 1,430 \times 10^{-7}$ m²/s, and differs in thermal conductivity by 5% from the value of 0.599 W/m °C.

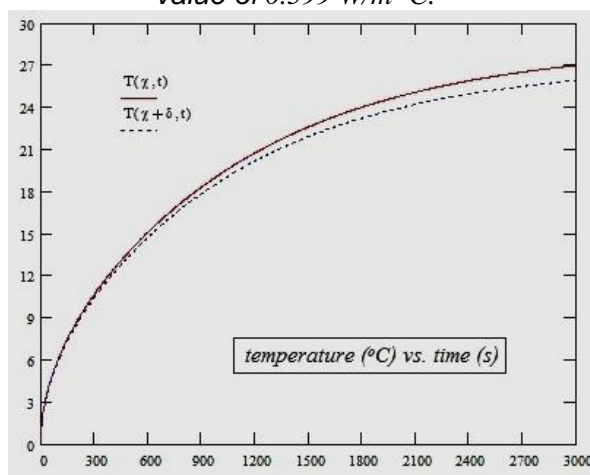


Figure 5. Temporal dependence of the temperature on the frontal surface ($x = l$) for two samples, whose thermal conductivities differ from each other by 5%. Theoretical data.

However, it depends on the value of the temperature T_{es} and the time during which it is possible to measure, considering that the temperature of the sample for the reasons given above should not exceed by more than a few degrees (5 - 10 °C) the initial temperature and, on the other hand, must be measured for a longer time than is necessary for the temperature difference to exceed that which can be detected with the available temperature sensor. Therefore, the limits of the useful time interval for the measurement, and thus the resolution of the method, are determined by the resolution of the temperature sensor itself and by the value of T_{es} .

It follows that: the choice of the temperature sensor as well as the magnitudes involved in expression (21) depend on the minimum differences in thermal conductivity or diffusivity to be detected.

3.2. Hamilton and Crosser's Model

The model of Hamilton and Crosser (Hamilton and Crosser, 1962), like that of Maxwell (Maxwell, 1881) and others, predicts the value of effective thermal conductivity of a medium in whose sine can be found particles scattered in a random and homogeneous way, which are sufficiently away from each other so that it is possible to neglect the interactions between them. According to this model, the effective thermal conductivity is expressed by:

$$\chi_f = \chi_{fb} \left(\frac{\psi + (v-1) - (v-1) \cdot (1-\psi) \cdot \lambda}{\psi + (v-1) + (1-\psi) \cdot \lambda} \right) \quad (\text{Eq. 25})$$

where: $\psi = \frac{\chi_n}{\chi_{fb}}$ is the relationship between the thermal conductivities of the particles and the medium respectively, λ is the volume fraction occupied by the particles in the fluid, v is a form factor, which takes into account the geometry of the particles. The subscripts n and fb represent the particles and the medium respectively.

Considering the equation (25) and that the effective specific heat capacity is expressed by:

$$\rho c_f = (1-\lambda) \cdot \rho c_{fb} + \lambda \cdot \rho c_n \quad (\text{Eq. 26})$$

It is set for thermal diffusivity, the following relation:

$$\alpha_f = \frac{\chi_{fb} \left(\frac{\psi + (v-1) - (v-1) \cdot (1-\psi) \cdot \lambda}{\psi + (v-1) + (1-\psi) \cdot \lambda} \right)}{(1-\lambda) \cdot \rho c_{fb} + \lambda \cdot \rho c_n} \quad (\text{Eq. 27})$$

If the medium in which the particles are found is a fluid, then the expressions for thermal conductivity and diffusivity in (20) are as follows:

If the medium in which the particles are found is a fluid, then the expressions for thermal conductivity and diffusivity in (20) are as follows:

$$\chi_{ef} = \mu \cdot \chi_{fb} \left(\frac{\psi + (v-1) - (v-1) \cdot (1-\psi) \cdot \lambda}{\psi + (v-1) + (1-\psi) \cdot \lambda} \right) + (1-\mu) \cdot \chi_p \quad (\text{28})$$

and

$$\alpha_{ef} = \frac{\mu \cdot \chi_{fb} \left(\frac{\psi + (v-1) - (v-1) \cdot (1-\psi) \cdot \lambda}{\psi + (v-1) + (1-\psi) \cdot \lambda} \right) + (1-\mu) \cdot \chi_p}{\mu \cdot [(1-\lambda) \cdot \rho c_{fb} + \lambda \cdot \rho c_n] + (1-\mu) \cdot \rho c_p} \quad (\text{29})$$

where the subscript p represents the sample holder.

Figures 6, 7, 8 and 9 show the relative variations of thermal conductivity and diffusivity as a function of the volumetric fraction according to (28) and (29) respectively.

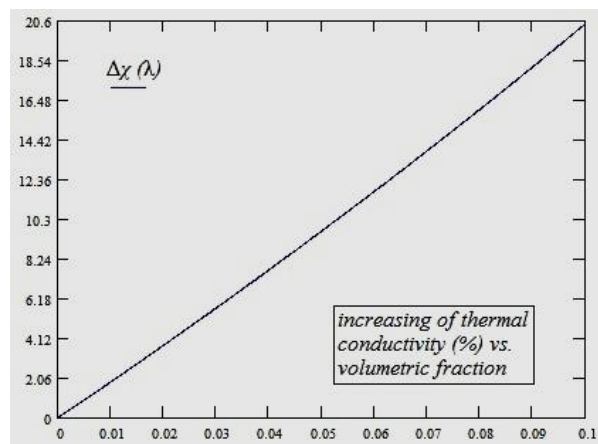


Figure 6. Increasing the thermal conductivity vs. volumetric fraction.

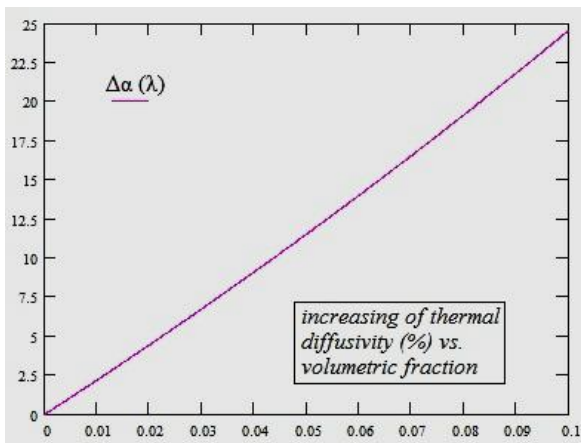


Figure 7. Increasing the thermal diffusivity vs. volumetric fraction.

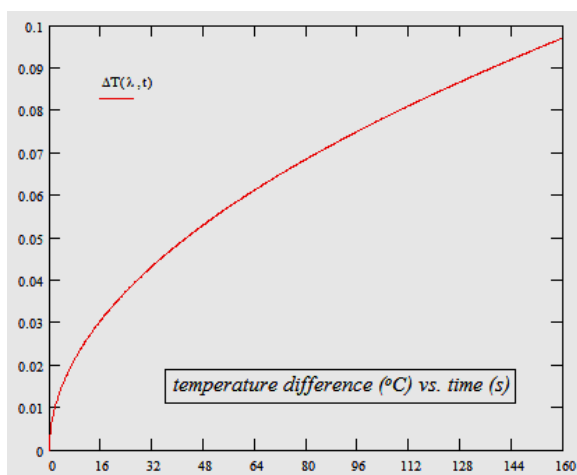


Figure 8. Temperature difference as a function of time, for an increase of the volumetric fraction by 1%.

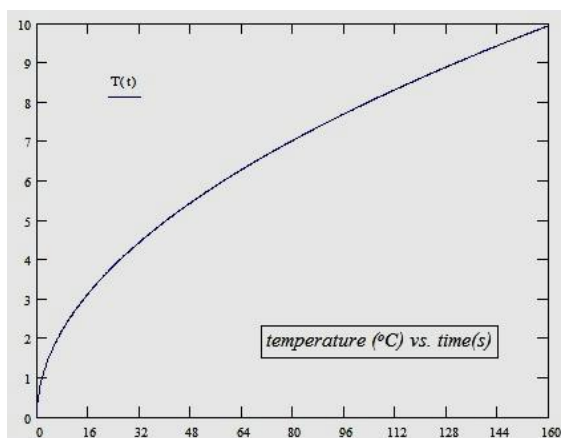


Figure 9. Temperature as a function of time. If we have as sample water with aluminum particles immersed in it and that the material of the sample holder is glass.

Figure 8 shows the temperature difference as a function of time $\Delta T(t)$ when the volume fraction of aluminum in water varies by 1%, assuming that we have, as a sample, aluminum

nanoparticles immersed in distilled water in a glass holder.

For them the values of thermal conductivity and specific heat capacity are as follows: $\chi_n = 211.015 W^{\circ}C^{-1}m^{-1}$, $\chi_{fb} = 0.599 W^{\circ}C^{-1}m^{-1}$, $\chi_p = 0.837 W^{\circ}C^{-1}m^{-1}$, $\rho_{c_n} = 2.453 \times 10^6 J^{\circ}C^{-1}m^{-3}$, $\rho_{c_{fb}} = 2.187 \times 10^6 J^{\circ}C^{-1}m^{-3}$, $\rho_{c_p} = 1.998 \times 10^6 J^{\circ}C^{-1}m^{-3}$. Figure 9 represents, for a similar sample, the behavior of the temperature as the time $T(t)$ elapses.

To verify the validity or not of the HC model, it is enough to measure the thermal diffusivity values of several samples that differ only in the value of their volumetric fraction and then verify that the expression (29) fits sufficiently well with the experimental points resulting from the measurements. If one wishes to study the behavior of a nanofluid, then proceed as above. To perform this type of study using the proposed method, it is necessary to choose the temperature sensor properly, because the resolution of the temperature must be in accordance with the minimum differences in thermal conductivity or diffusivity that need to be detected.

CONCLUSIONS:

The heat diffusion equation was solved for the conditions of the proposed method, obtaining an expression from which it is possible to determine both thermal conductivity and diffusivity values. The choice of the temperature sensor as well as the magnitudes involved in expression (21) depends on the minimum differences between conductivities and thermal diffusivity to be detected, as illustrated in figures 4 and 5. In this case, a sensor with a precision of up to one hundredth of a second is required. If it were less precise, it would be necessary to measure it for a longer time (about one hour). This would increase the temperature in the sample considerably, giving rise to the phenomenon of conduction of heat by radiation, which is not desired.

To measure in solid materials, it is necessary to use a material that can be prepared into rods, cylindrical or of another geometry. The method allows to check the HC model, provided that it has a temperature gauge with a resolution that allows it to differentiate up to the hundredth of a degree centigrade.

REFERENCES:

1. Fox, J. N., McMaster, R.H. Measurement of the thermal properties of a metal using a relaxation method, *American Journal of Physics*, **1975**, 43, 1083- 1086.
2. Ficker, T. A non-stationary method for the measurement of the thermal conductivity of solids in student laboratories, *European Journal of Physics*, **1996**, 17, 307-310.
3. Hurley, D. H., Schley, R. S., Khafizov, M. and Wendt, B. L. Local measurement of thermal conductivity and diffusivity, *Review of Scientific Instruments*, **2015**, 86, 123901- 123901-8.
4. Koblinski, P., Phillpot, S.R., Choi, S.U.S., Eastman, J.A. Mechanisms of heat flow in suspensions of nano-sized particles (nanofluids), *International Journal of Heat and Mass Transfer*, **2002**, 45, 855- 863.
5. Xue, Q., Xu, W. M. A model of thermal conductivity of nanofluids with interfacial shells, *Materials Chemistry and Physics*, **2005**, 90, 298- 301.
6. Gregorová, E. The thermal conductivity of alumina–water nanofluids from the viewpoint of micromechanics, *Microfluidics and Nanofluidics*, **2014**, 16, 19- 28.
7. Xuan, Y., Li, Q. Heat transfer enhancement of nanofluids, *International Journal of Heat and Fluid Flow*, **2000**, 21, 58- 64.
8. Putnam, S. A., Cahill, D. G., Braun, P. V., Ge, Z., Shimmin, R. G. Thermal conductivity of nanoparticle suspensions, *Journal of Applied Physics*, **2006**, 99, 084308.
9. Eastman, J. A., Choi, S. U. S., Li, S., Yu, W., Thompson, L. J. Anomalous increased effective thermal conductivities of ethylene glycol-based nanofluids containing copper nanoparticles, *Applied Physics Letters*, **2001**, 78, 718.
10. Choi, S. U. S., Zhang, Z. G., Yu, W., Lockwood, F. E., Grulke, E. A. Anomalous thermal conductivity enhancement in nanotube suspensions, *Applied Physics Letters*, **2001**, 79, 2252.
11. Xie, H., Wang, J., Xi, T., Liu, Y. Thermal Conductivity of Suspensions Containing Nanosized SiC Particles, *International Journal of Thermophysics*, **2002**, 23, 571– 580.
12. Klingenberg, D. J., Venerus, D. C. Thermal Conductivity Measurements in Nanofluids, *American Institute of Chemical Engineers*, **2006**, 06AIChE.
13. Zhang, X., Gu, H., Fujii, M. Effective thermal conductivity and thermal diffusivity of nanofluids containing spherical and cylindrical nanoparticles, *Journal of Applied Physics*, **2006**, 100, 044325 - 044325-5.
14. Hamilton, R. L., Crosser, O. K. Thermal Conductivity of Theory of Heterogeneous Two-Component System, *Industrial & Engineering Chemistry Fundamentals*, **1962**, 1, 187- 191.
15. Maxwell, J.C. A Treatise on Electricity and Magnetism, 2nd ed, *Clarendon Press*, 435, Oxford, UK, 1881.
16. Shemeena, N., Rajesh, B., Kurian, A., George, S. D. Thermal conductivity measurement of organic solvents incorporated with silver nanoparticle using photothermal techniques, *International Conference on Materials Science and Technology*, India 2012.
17. González, M. E., Denis, A. Soba, A. Modelización de la conductividad térmica del UO_2 y $(\text{U,Gd})\text{O}_2$ bajo irradiación. Implementación en el código Dionisio, *ANALES AFA*, **2014**, 25, 211-213.
18. Warriar, A. R., Jayakrishnan, R., John, T. T., Kartha, C. S., Vijayakumar, K. P. Study on optical, electronic and thermal properties of $\beta\text{-In}_2\text{S}_3$ thin films using photothermal beam deflection technique, *J Mater Sci: Mater Electron*, **2015**, DOI 10.1007/s10854-015-4201-y.
19. Martínez, K., Marín, E., Glorieux, C., Lara, A., Calderón, A., Peña, G., Ivanov, R. Thermal diffusivity measurements in solids by photothermal infrared radiometry: Influence of convection-radiation heat losses, *International Journal of Thermal Sciences*, **2015**, 98, 202-207.
20. Cobirzan, N., Balog, A. A., Belean, B., Borodi, G., Dadârlat, D., Streza, M. Thermophysical properties of masonry units: Accurate characterization by means of photothermal techniques and relationship to porosity and mineral composition, *Construction and Building Materials*, **2016**, 105, 297–3.